Cement and Concrete Research 38 (2008) 1365–1373

Contents lists available at ScienceDirect

Cement and Concrete Research

journal homepage: http://ees.elsevier.com/CEMCON/default.asp

Accelerated carbonation of cement pastes in situ monitored by neutron diffraction

M. Castellote [a,*], C. Andrade [a], X. Turrillas [a], J. Campo [b], G.J. Cuello [c]

[a] Institute of Construction Science "Eduardo Torroja", IETcc, (CSIC), Madrid, Spain
[b] Institute of Materials Science of Aragón, ICMA, (CSIC), Zaragoza, Spain
[c] Institute Laue Langevin (ILL), Grenoble, France

ARTICLE INFO

Article history:
Received 10 July 2007
Accepted 11 July 2008

Keywords:
Accelerated carbonation
In situ monitoring
Neutron diffraction
Phase analysis
Microstructure changes

ABSTRACT

In-situ monitoring of the changes that take place in the phase composition of cement pastes during accelerated carbonation (100% CO_2) for different binders, has been carried out, by taking Neutron Diffraction patterns in parallel with the carbonation experiments. The variation of the intensity of chosen reflections for each phase along the experiment has been used to monitor concentration changes and has supplied data, in real time, for fractional conversion of different phases (Portlandite, Ettringite and CSH gel) of the hydrated cement pastes. Fitting of these results has allowed to make a qualitative approach to the kinetics of the carbonation of the different phases and extracting conclusions on the microstructural changes that takes place during the carbonation of cement pastes.

1. Introduction

One of the most important depassivation mechanisms of steel reinforcement in concrete is that caused by the neutralisation of the cement matrix. For this reason, the carbonation of concrete, as consequence of its interaction with the atmospheric CO_2, has been considered for years a subject of interest in researches of cement chemistry [1]. The process known as carbonation, is a complex physicochemical process that slowly modifies the structure of the concrete in the course of time and induces changes into its chemical [2–14] and physical [15–21] properties.

In spite of this large number of studies, there are still not answered questions, which are of crucial importance for the sake of modelling the process [22–30]. For example, although it has been shown that porosity decreases in OPC pastes, due to the production of calcium carbonate, it has not been quantified this decrease and it has not been determined the controlling parameters of this effect. On the other hand, it is known that not only Portlandite gets carbonated during the process [3,4,26,31]. However there is a lack of knowledge on the relative fractional conversion of the different phases as the process goes on. Therefore, techniques which are able to give results enabling access to this kind of questions are of great importance for the progression of the understanding of the carbonation process. One of these advanced techniques, giving thorough information, is the neutron diffraction technique, as neutrons penetrate deep into the matter providing information about the bulk of the sample, what makes them a very useful tool to understand how the material changes and degrades. They are able to give information on the crystalline phases of the matrixes, and by indirect deductions, also about amorphous phases.

Present paper reports on the phase analysis and microstructure changes recorded by in situ, (that is, while the reaction is progressing) by simultaneous acquisition of neutron diffraction during experiments of accelerated carbonation of cement pastes. Although the CO_2 gas concentration used has been of 100% and it might be claimed that it modifies the carbonation rate, carbonation at lower concentration does not allow to record the microstructural changes in the lapse of several hours, that is the reasonable allowable time for neutron experiments. Concentrations of CO_2 of 5% or lower would take days to produce carbonation even in a few mm at the surface of any monolithic specimen and therefore, making unpractical the study in-situ of the carbonation process. In addition to the samples cast with deuterated water and carbonated during the Neutron Diffraction experiments, other set of samples was cast with ordinary water and also fully carbonated with CO_2 gas at 100% in carbonation chambers. This second set was used for complementary tests.

2. Experimental procedures

2.1. Materials and preparation of specimens

Two different series of specimens were prepared:

Series a) For the in-situ carbonation experiments. Cement pastes (with three different types of binder) were prepared by hand mixing the cements with deuterated water from 99.95% purity to a w/c ratio of 0.5.

Series b) For obtaining the complementary data, equivalent samples to those of the point a) were cast with ordinary water, at the same w/c ratio, and were similarly carbonated in carbonation chambers at the laboratory.

* Corresponding author.
E-mail address: martaca@ietcc.csic.es (M. Castellote).

0008-8846/$ – see front matter © 2008 Elsevier Ltd. All rights reserved.
doi:10.1016/j.cemconres.2008.07.002

Table 1
Chemical analysis of the cement, fly ash and micro-silica used

	SiO_2	Al_2O_3	Fe_2O_3	CaO	MgO	SO_3	Cl^-	Na_2O	K_2O	free CaO
Cement	20.2	2.37	4.1	65.84	1.85	3.8	0.02	0.11	0.65	1.5
Fly ash	48.71	25.18	5.18	12.09	1.61	0.43	–	0.61	3.28	0.15
Micro-Silica	96.32	0.00	–	0.67	0.49	–	–	0.15	0.39	0.04

Series a) and b) consisted of pastes with three different types of binders. The first binder was plain OPC cement type CEM I 42.5 R sulphate-resistant, having a 5% of addition of lime. The second one, mix OPC-FA, was prepared using the same cement substituted in a 35% by fly ash. For the third type, mix OPC-MS, was used again the same cement with a substitution of a 10% by micro-silica. The chemical analyses of the Cement, Fly Ash and Micro-Silica, are given in Table 1.

These paste specimens were cast in cylindrical plastic moulds, which were sealed, in order to avoid carbonation, and allowed to cure for 28 days at room temperature (22 °C) in a humid chamber at a relative humidity, RH, higher than 95%. The resulting specimens were cylindrical, 9 mm ϕ and 32 mm height.

2.2. Techniques and procedures

2.2.1. Series a)

After curing and demoulding, the deuterated specimens of every mix were kept sealed, in order to avoid carbonation, until the in-situ experimental trials, that took place 130 days after casting them.

The experimental set up for the in situ experiments is shown in Fig. 1, where a scheme and a photo of the test device are given. A glassed mini-carbonation-chamber was designed, consisting in a cylindrical body with a tube and a valve in its bottom. It has a perforated glass separating the body of the device and the valve that allows filling in the bottom part with the » 65% RH regulation solution (saturated solution of $NaNO_3$) keeping it separated from the specimen. The device has a hermetic cap, where the sample was suspended, with three inlets (inlet of CO_2, outlet of CO_2 and aeration). The CO_2 gas was delivered at a concentration of 100%, through a tube, covered by a sheet of cadmium (for avoiding interferences of the plastic tube with the neutrons), at the bottom of the cylindrical device, in order to assure the right circulation of the gas through the sample (see Fig. 1).

The in-situ carbonation was followed on line by simultaneous acquisition of diffraction patterns at the D20 instrument of the Institute Max von Laue – Paul Langevin (ILL), in Grenoble, France. The neutron diffraction data were collected by continuously storing the detector counts, every 300 s, exploring an angular domain in 2θ from 10° to 150°. The neutron beam had a rectangular section of 10 mm width × 30 mm height, covering all the perimeter of the sample. To calibrate the wavelength used, a powder of Si furnished by the NBS (National Bureau of Standards) was used. The diffraction pattern of this standard was refined by Rietveld analysis and a wavelength of 1.321 Å was found. This wavelength was used in the subsequent measurements.

The powder diffraction patterns have been analysed by a standard procedure. Crystalline phases were identified by a search–match manual procedure and selected peaks for Portlandite, Calcite, Ettringite and a Calcium silicate hydrate were fitted to Gaussian curves for the whole series. The variation of intensity of a chosen reflection for a particular phase along the experiment (related with the concentration) has been used to monitor concentration changes.

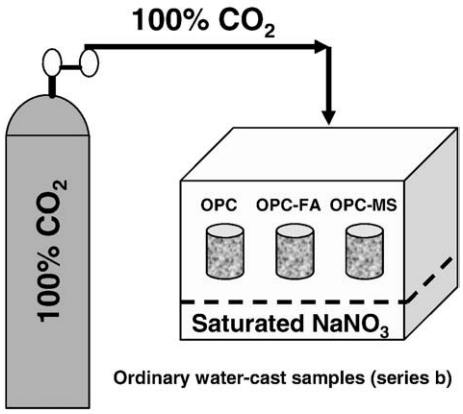

Fig. 2. Experimental set up for the laboratory carbonation experiments in a chamber at the 100% CO_2 concentration for specimens of series b).

2.2.2. Series b)

Paste specimens prepared with ordinary water, for the three binders, were introduced in a 100% CO_2 concentration chamber (Fig. 2). In this chamber, the specimens were allowed to equilibrate at a relative humidity RH of about a 65% and 22 °C by means of a saturated solution of $NaNO_3$ and they were submitted to accelerated carbonation during 103 days. After this time, the state of carbonation was analysed according to the phenolphthalein tests. For this series,

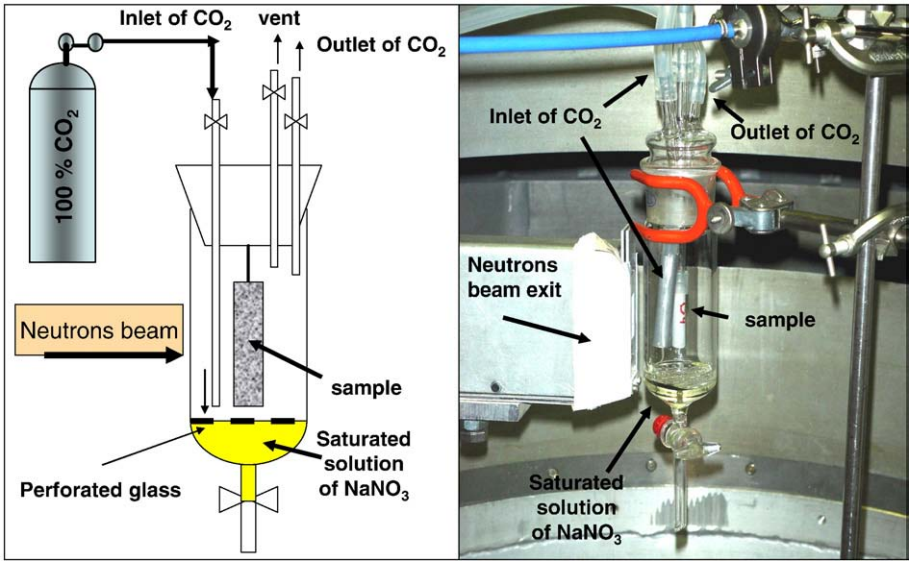

Fig. 1. Experimental set up for the in situ carbonation experiments, at the 100% CO_2 concentration for specimens of series a).

Table 2
Summary of the samples cast and the test performed with the different mixes

Series	Mix	Casting Water[a]	Experiment[b]	% CO_2	Time of carbonation (days)	Final state[c]	Comments[d]
a)	OPC OPC-FA OPC-MS	D	IS–ND	100	0.375 0.382 0.538	PC	Fractional conversion data
b)	OPC OPC-FA OPC-MS	O	–	–	–	NC	Phen MIP TG
	OPC OPC-FA OPC-MS	O	LC	100	103	CC	Phen MIP TG

[a] D: Deuterated water; O: Ordinary water.
[b] IS-ND: in situ Neutron Diffraction, LC: Laboratory chamber.
[c] NC: No Carbonated; PC: Partially Carbonated; CC: Completely Carbonated.
[d] Phen: phenolphthalein tests; MIP: Mercury Intrusion Porosimetry, TG: Thermogravimetry.

samples of every mix, before and after the carbonation treatment, were characterised by Thermogravimetry (TG) and Mercury Intrusion Porosimetry (MIP).

A summary of the samples cast and the test performed for the different mixes is presented in Table 2.

3. Results

3.1. Series a) Neutron diffraction patterns

In Fig. 3, as an example of the diagrams obtained, the neutron diffraction patterns of the accelerated carbonation experiment for the OPC sample, covering the interval from 21°–35° in 2θ, are presented. Fig. 3-a shows the diffraction patterns in the form of a tri-dimensional surface plot. In Fig. 3-b, the contour map for the diffraction data is sketched, where data are displayed as the projection (in the 2θ-time plane) of a pseudo three-dimensional map obtained after sequentially connecting the diffraction patterns. Both types of plots allow the observation of the major features of the whole experiments, i.e., the phases existence domains and their growing and decaying.

The analysis of the neutron diffraction patterns, in the range from 10° to 150° 2θ, has allowed the identification of 4 main crystal phases: Portlandite, Calcite, Ettringite, and a form of crystalline Calcium Silicate Hydrated (CSH gel). No anhydrous cement was clearly resolved as some peaks are overlapped with that of other phases, mainly Calcite, and for that not overlapped, not clear peaks were detected. In Fig. 4, for the sake of clarity, only a section of the diffraction patterns is depicted and selected peaks of these phases, chosen by their isolation and intensity, are marked for the initial and final pattern for the three mixes.

These peaks have been fitted to Gaussian curves for the whole series. This was done with procedures written in IDL code using the Marquart algorithm. The variation of intensity of a chosen reflection for a particular phase along the experiment (related with the concentration) was used to monitor concentration changes. Fig. 5 (a–d), shows the evolution of the normalised intensity as a function of the time of carbonation for the three different mixes and the four crystalline phases analysed. In Fig. 5, it can be seen that carbonation implies the simultaneous reduction of the Portlandite, Ettringite and CSH gel while Calcite increases progressively (note that the initial normalised intensity for Calcite is not zero due to an initial amount of lime in the cement).

It has to be pointed out that the biggest peaks, corresponding to Portlandite and Calcite, present a very small bias in the fit (the error bars in Fig. 5 represent the 95% confidence limits) while the peaks corresponding to Ettringite presents higher dispersion, reaching a point in which the resolution of the peaks do not allows fitting them. This is the case for the peak corresponding to the CSH gel, which is very close to the biggest peak of Calcite. That is why it has been only possible to fit it, in some extent, for the OPC mix.

In a diffraction experiment, we can distinguish two kinds of contributions to the differential cross section: the coherent and incoherent terms. The former is proportional to the structure factor (which is Q-dependent and contains the information about the structure of the sample) and to the coherent scattering cross section. The latter is proportional to the incoherent scattering cross section and is independent of the momentum transfer. It means that a diffraction spectrum is composed of two terms, the one containing the Bragg peaks plus a constant term due to the incoherent scattering. The

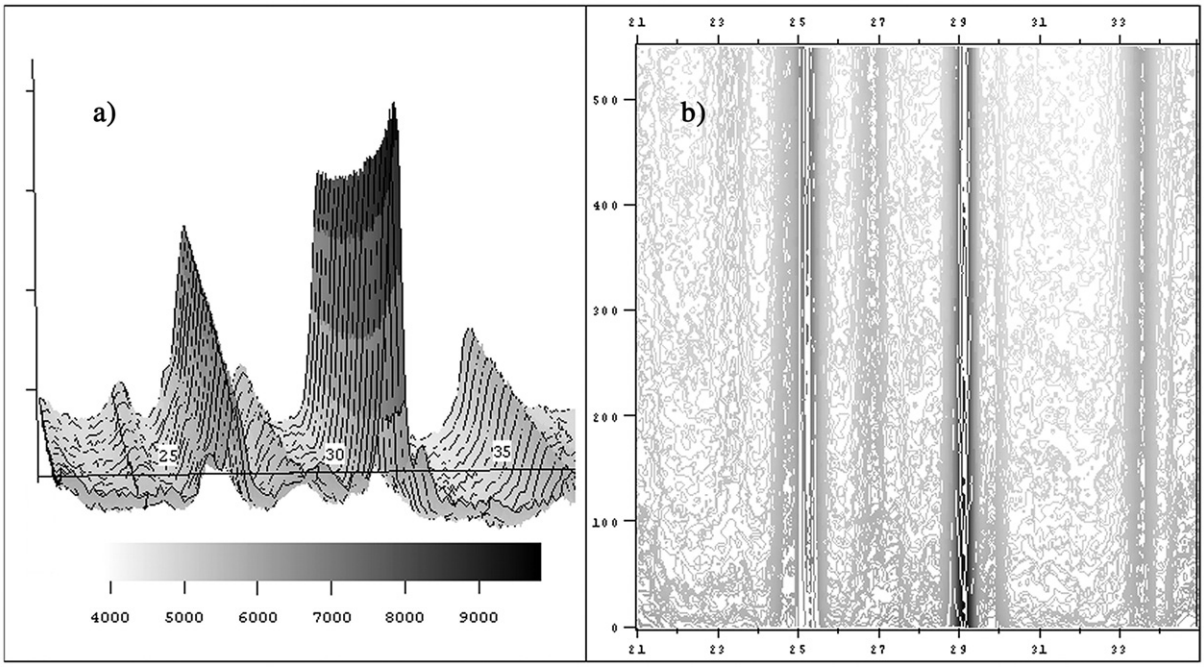

Fig. 3. Neutron diffraction patterns of the accelerated carbonation experiment for the OPC sample, covering the interval from 21°–35° in 2θ. a) Surface plot, b) Contour map.

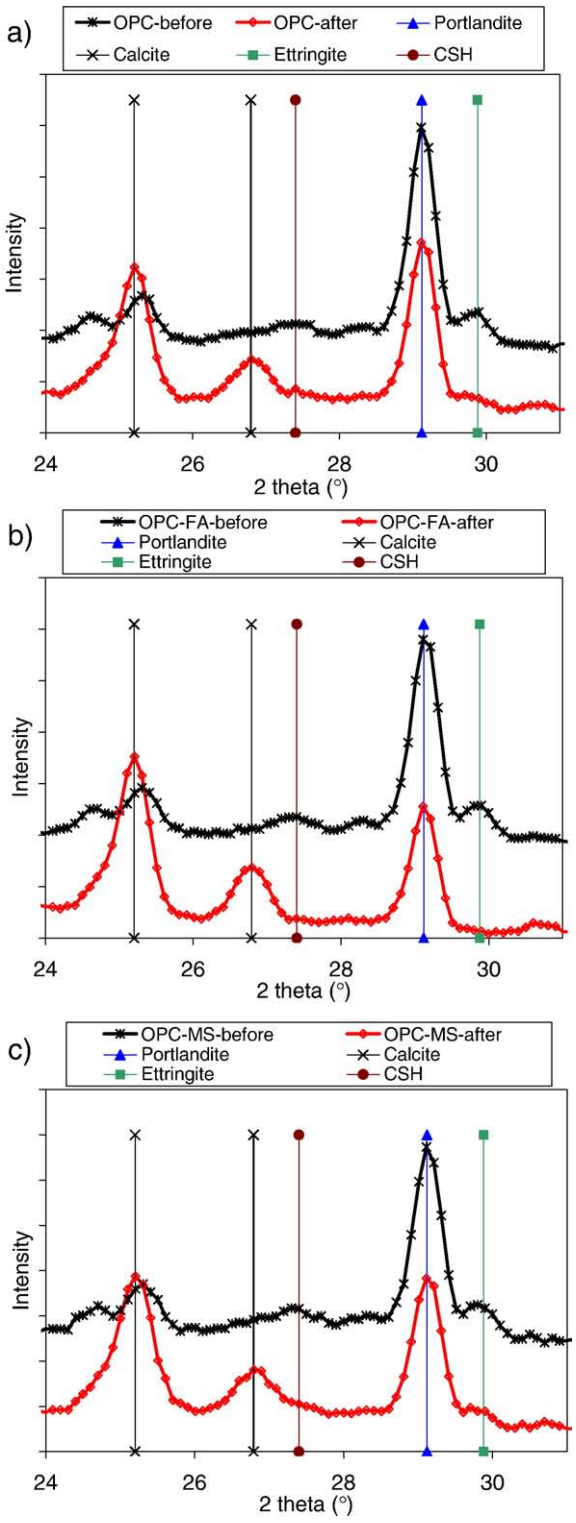

Fig. 4. (a–c): Section of the initial and final diffraction patterns for the three mixes (the selected peaks of the different phases have been marked). a) OPC, b) OPC-FA, c) OPC-MS.

coherent and incoherent scattering cross sections are intrinsic properties of the nuclei and their values are tabulated [32]. In the particular case of the hydrogen the incoherent and coherent cross sections are 80.26 barns and 1.7568 barns, respectively (1 barn = 10^{-24} cm^2). These numbers are to be compared with usual values for other nuclei: ~1 barn and ~7 barns for incoherent and coherent contribution. Therefore, in comparison with other systems, the hydrogen gives a huge constant incoherent signal (seen as background in a diffraction experiment) and a small coherent signal [33].

Therefore, the background can be related to the hydrogen amount, so to the water fraction in the sample, not only free water, but also combined water in the hydrates. The integration of a fraction of the diffraction patterns backgrounds as a function of the time of carbonation (normalised intensity to unity at the low 2θ region, where no peaks appear), is presented in Fig. 6. In Fig. 6 it can be observed that the background decreases during the carbonation experiment, following the same trend that the carbonation of the different phases (see Figs. 4 and 5) which implies a loss of water during the experiment that is removed from the system due to the control in the RH with the $NaNO_3$ solution. In the case of the sample OPC-FA, there is a point in the experiment in which there is a stabilisation of the background, which has been attributed to the higher initial rate of carbonation for this sample, with formation of more water and reaching a moment in which the rate of carbonation is more or less the rate of evacuation of the formed water. More research is carrying out in order to clarify this point.

3.2. Series b)

3.2.1. Thermogravimetry analysis

The results obtained from Thermogravimetry Analysis, TG, for the initial samples and for the specimens submitted to complete carbonation at 100% CO_2 are presented in Fig. 7, where, as expected, differences between the different samples, mainly for the amount of Portlandite can be observed. In addition, it can be seen that the total loss of weight becomes higher in the carbonated samples due to the uptake of CO_2, that it is later released during the TG test.

The loss of weight at specified temperatures allows the quantification of the amounts of Portlandite and Calcite in each sample. Loss of bound water (105 °C ~ 425 °C), which derives mainly from calcium silicate hydrate but includes contributions from aluminate and ferroaluminate hydrates [1,31,34] has also been quantified. The calculated values are given in Table 3, where the percentages are referred to the initial weight of the paste. According to the data in Table 3, there is not any trace of Portlandite in any of the carbonated samples and, as expected, the amount of combined water decreases significantly when carbonating. It is worth pointing out again that the values of percentage of Calcite in the reference samples are due to inclusion of a 5% of limestone in the cement, as they kept carefully sealed, in order to avoid carbonation.

In agreement with this data, the phenolphthalein test after carbonation showed all the samples fully carbonated.

3.2.2. Mercury Intrusion Porosimetry

The results obtained from Mercury Intrusion Porosimetry for the initial samples (before carbonation) and for the specimens carbonated completely in the laboratory chamber, using 100% CO_2 during 103 days, are presented in Fig. 8 (a–b), where the total porosity (percent in volume) and the bulk density of the matrixes, are given. In Fig. 8, it can be seen that, as already known, the carbonation treatment induces, in all the samples, a decrease in the total porosity, and therefore, denser samples. The percentages of reduction for each sample are also given in Fig. 8-a, where it can be deduced that the higher reduction has taken place for the sample with addition of micro silica, OPC-MS, and the smaller one for the OPC-FA sample.

A more detailed analysis can be made by looking at the differential pore size distributions for the different samples, as presented in Fig. 9.

Fig. 9 shows that the pore size distribution is a bit different for the different types of pastes. Before the process of carbonation, all of them present two maxima, being the smallest one at about 0.3 μm and the biggest one around 0.05 μm. For the pores smaller than 0.05 μm, the lower values of pores are in the sample OPC-MS while OPC-FA presents the higher values of pores. After carbonation, the maxima of

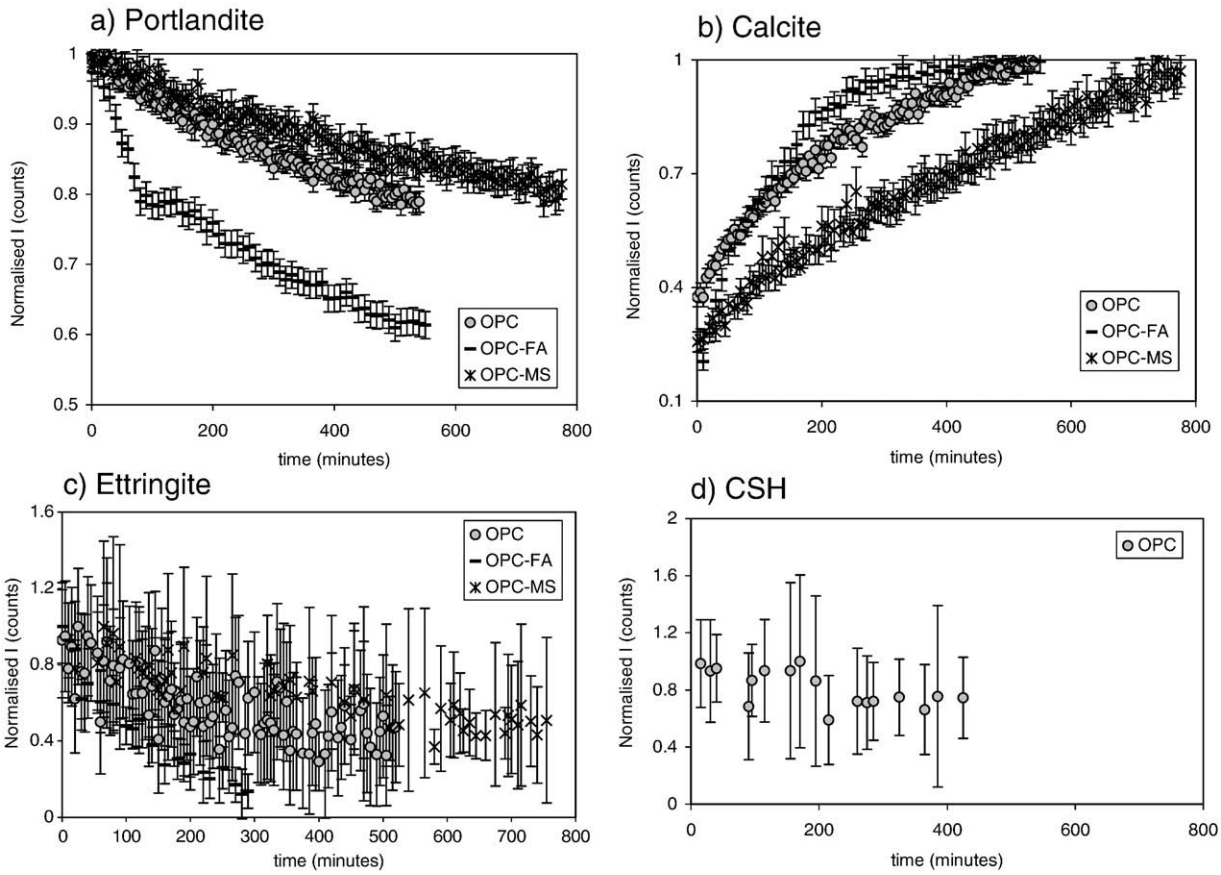

Fig. 5. (a–d). Evolution of the normalised intensity as a function of the time of carbonation for the three different mixes and the four crystalline phases analysed. (The error bars represent the 95% confidence limits).

about 0.3 μm disappear for every sample, and that at 0.05 get shifted towards lower sizes en the case of OPC and OPC-MS and towards higher ones for OPC-FA, presenting, in every case, smaller absolute values.

4. Discussion

In the carbonation process, the CO_2 gas penetrates through the empty spaces of the concrete pore network and dissolves in the pore solution where reacts with the Ca^{2+}/OH^- ions to precipitate $CaCO_3$ that has a very low solubility product. As Ca^{2+}/OH^- ions are removed from the solution by carbonation, precipitated Portlandite is progressively dissolved, inducing a buffering action. However, carbonation implies not only the reduction of Portlandite but also of other phases of the cement paste, as Ettringite and CSH gel, while Calcite increases progressively. The simultaneous carbonation of Portlandite and CSH had been reported elsewhere [3,31,34], and here it is clearly noticed, as depicted in Fig. 10, where the fractional conversion of the different phases is given, (taking out the error bars, for the sake of clarity) for the different mixes analysed. The experimental data have been fitted empirically (solid lines in Fig. 10), allowing to make a qualitative approach to the kinetics of the carbonation of the different phases. The corresponding relationships are given in Table 4.

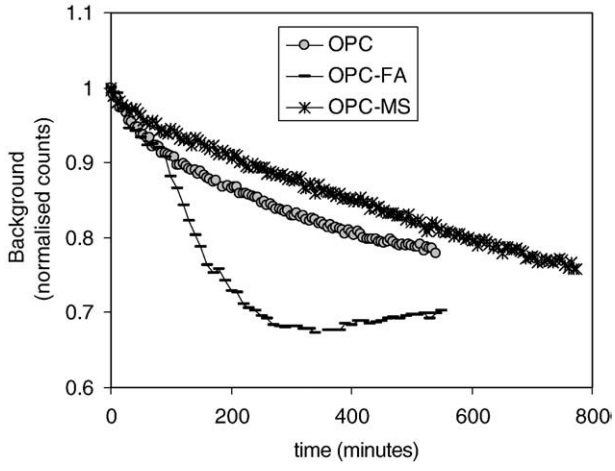

Fig. 6. Evolution of the background, at low 2θ, during the carbonation experiments.

From Table 4 it can be seen that all the phases that are consumed by the carbonation process (Portlandite, Ettringite and CSH) disappear according to an exponential decay of first order, while formation of Calcite follows the trend of a sigmoidal shape given by a Boltzman function, being the rate of change of each phase different.

This can be clearly seen by looking carefully at the constants t1, from the fitting equations, that represent the temporal decay parameters, being slower the process as higher is the constant. These constants have been depicted in Fig. 11 for the different phases, consumed in the process, and mixes. From them, it can be deduced that even though for the same mix, the rate for the different phases is different, there is more or less the same proportionality between each phase in the different samples. So, Ettringite is the phase that consumes quicker then, the CSH gel, at least the crystalline fraction, being the consumption of Portlandite, as long as the different phases are concerned, the slowest process. Therefore, considering that carbonation is a continuous process and that the definition of carbonated region is arbitrary, it is suggested the definition as the region without Portlandite, as used in [31], as quite reliable.

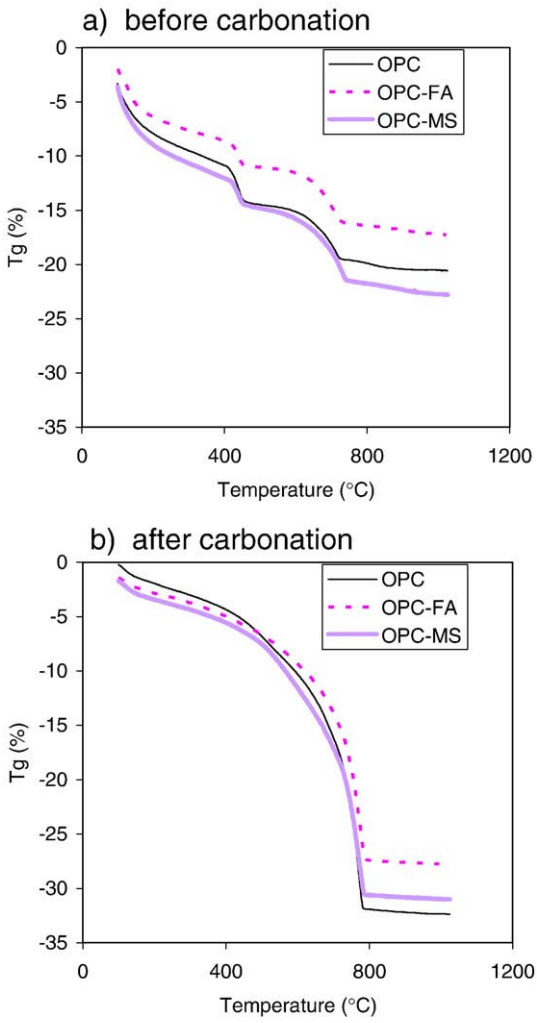

Fig. 7. (a–b). Thermogravimetry Analysis (TG) of the samples. a) before and b) after full carbonation at 100% CO_2.

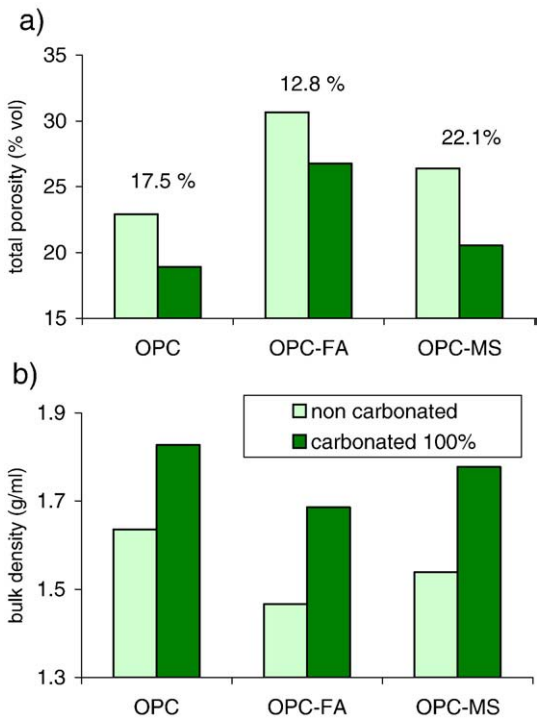

Fig. 8. (a–b): MIP microstructure parameters before and after full carbonation at 100% CO_2. a) Total porosity (percent in volume); the percentages of reduction for each sample are also given. b) Bulk density.

On the other hand, concerning the different mixes, the slowest process takes place for the paste including micro-silica in their composition, and that of fly ashes is the quickest one, which cannot be related to the porosity of the samples, neither before nor after full carbonation at 100% CO_2 (see Fig. 8).

In addition, new formed Calcite due to the carbonation process presents some differences with the Calcite initially present in the samples. For analysing them, from the in-situ data, on one hand, the evolution in the volume of the unit cell of Calcite has been calculated. Provided that Calcite crystallises in the trigonal system (Space Group *R-3C* [35], at least two independent reflections corresponding to a different family of planes are necessary [36] for making the calculations (in this case (1 1 3) and (0 0 6) have been used).

On the other hand, the full width at half maximum (FWHM) of the fitted Gaussians has also been determined. This parameter can be related to crystal size: the smaller the FWHM of the peaks, the larger are the crystallites of the phase, or better the crystallinity degree. The results are given in Fig. 12 (a–b) respectively, where it has been deduced that the new formed Calcite increases the size of the unit cell (see also the shifts of the position in the peaks of Calcite towards lower angles in Fig. 4 in about a 0.4%, and is less crystalline than the original one, especially in the case of the cement with additions.

Concerning the decrease in the porosity due to carbonation, calculations have been made with the different volumes of the unit cells for the different phases, taking into account the corresponding number of formula units per unit cell for each phase, corresponding to their specific crystal system group. These calculations have allowed to deduce that the conversion of Portlandite to Calcite implies an increase of a 12% in the volume of the solid phases.

Concerning Ettringite and the crystalline phase of CSH detected, taking into account only Calcite as the solid product formed, would imply a decrease of solid phases of about a 68% and 40% respectively. However, Ettringite and CSH not only give as solid product of carbonation Calcite, but also, SiO_2, Al_2O_3, …, that contribute also to the decrease of porosity. In addition, there is the amorphous CSH, for which these calculations are not possible.

Therefore, a direct relationship between the initial amount of Portlandite in the sample and the reduction in the porosity (% vol) due to carbonation was not found, as can be deduced from Fig. 13. However, it has been found another controlling parameter of the degree of carbonation: the "bound" water determined by TG analysis. Thus, in Fig. 13, it is shown that a good linear relationship has been found between the decrease in porosity and the percentage of bound water in the sample, which implies a strong relation between the initial CSH gel content and the carbonation degree.

Table 3
Percentages of bound water, Portlandite and Calcite in the different samples before and after carbonation at 100% CO_2

(%)	OPC		OPC-FA		OPC-MS	
	Before	After	Before	After	Before	After
Bound water	7.3	4.0	6.4	3.6	8.0	1.9
Porlandite	14.7	0.0	8.7	0.0	9.4	0.0
Calcite	11.2	51.8	10.9	43.4	13.8	49.6

5. Conclusions

In this paper, in-situ monitoring of the changes that take place in the phase composition of cement pastes during accelerated carbonation (100% CO_2) for different binders has been carried out, by taking

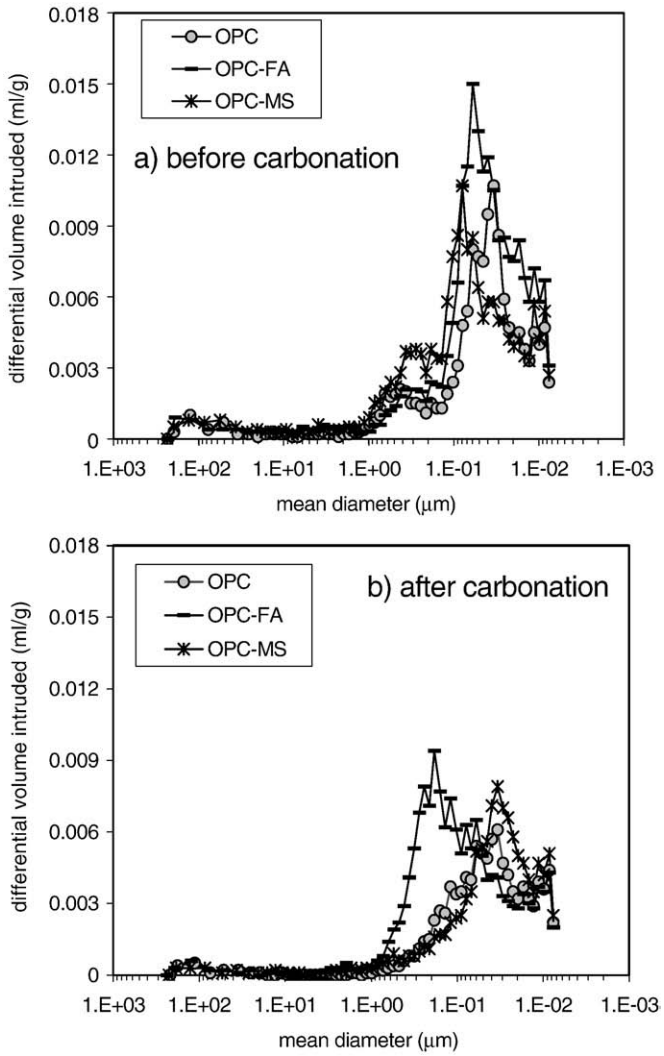

Fig. 9. (a–b). Pore size distribution in the samples. a) before and b) after complete carbonation at 100% CO_2.

simultaneous Neutron Diffraction patterns. The conclusions that can be drawn up are:

1) The ND technique has allowed the monitoring of the major features of the carbonation reactions, i.e., the phases existence domains and their growing and decaying: carbonation implies the simultaneous reduction of the Portlandite, Ettringite and CSH gel while Calcite increases progressively.
2) The variation of the intensity of a chosen reflection for a particular phase along the experiment (related with the concentration) has been used to monitor concentration changes and has allowed obtaining data, in real time, for fractional conversion of different phases of the reactants. Fitting of these curves has allowed making a qualitative approach to the kinetics of the carbonation of the different phases, deducing that all the phases consumed by the carbonation process disappear according to an exponential decay of first order, while formation of Calcite follows the trend of a sigmoidal shape given by a Boltzman function.
3) The rate of decrease of each phase is different for the different mixes. For the same mix, the rate for the different phases is different, but maintaining the same proportionality between each phase in the different samples. Ettringite is the phase that reacts quicker, then, the crystalline fraction analysed of the CSH gel, being the consumption of Portlandite, the slowest persistent process.
4) The slowest process takes place for the paste including micro-silica in their composition, and that of fly ashes is the quickest one, which is not related to the porosity of the samples, neither before and nor after full carbonation at 100% CO_2.
5) The new formed Calcite, due to carbonation, increases the size of its unit cell and is less crystalline than the original one, especially in the case of the cement with additions.
6) As expected, after full carbonation, all the samples are denser. From calculations related to the volume of the crystal phases and the relationship found between the percentages of reduction of porosity for each sample and the percentage of bound water in

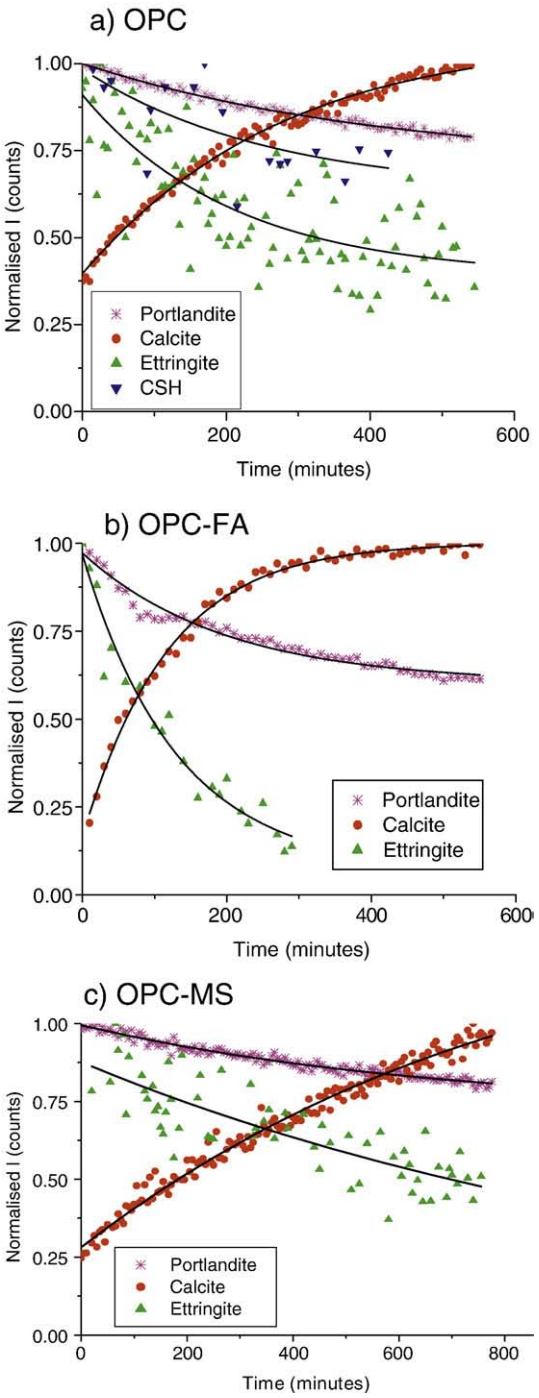

Fig. 10. (a–c): Fractional conversion of the different phases for the different mixes carbonated. a) OPC, b) OPC-FA, c) OPC-MS. (As solid lines, fitting of the data to the equations given in Table 4).

Table 4
Fitting of the fractional conversion of the different phases during the in-situ carbonation experiments

		OPC	OPC-FA	OPC-MS
PORTLANDITE: Exponential decay	$y0$	0.71	0.60	0.72
$y=y0+A1\ \exp(-x/t1)$	A1	0.29	0.37	0.27
	t1	427.73	197.44	673.15
	R^2	0.985	0.969	0.966
ETTRINGITE: Exponential decay	$y0$	0.389	0.07	0.410
$y=y0+A1\ \exp(-x/t1)$	A1	0.521	0.899	0.548
	t1	209.77	130.68	417.84
	R^2	0.611	0.966	0.712
CSH: Exponential decay	$y0$	0.63	–	–
$y=y0+A1\ \exp(-x/t1)$	A1	0.35	–	–
	t1	259.72	–	–
	R^2	0.443	–	–
CALCITE: Boltzman Function (Sigmoidal shape)	A1	−5.17	−14.44	−5.30
$y=A2+((A1-A2)/(1+\exp((x-x0)/t1)))$	A2	1.072	1.000	1.33
	$x0$	−525.57	−323.24	−1126
	t1	249.29	113.06	675.11
	R^2	0.990	0.994	0.984

Equations, parameters and correlation coefficients. (Graphical presentation in Fig. 10).

the sample, the main reduction in porosity has been attributed to the amorphous fraction of CSH gel.

Acknowledgements

The experiments reported here were done thanks to the beamtime (Exp 5-25-50) granted by the Institute Max von Laue- Paul Langevin (ILL). The authors are especially grateful to the staff of D20. The authors also acknowledge the funding provided by the Spanish MMA through the project n° 005/2006/2-3.1.

References

[1] G. Verbeck, Carbonation of hydrated portland cement, PCA Bull. 87 (1958) 17–36.
[2] Kazutaka Suzuki, Tadahiro Nishikawa, Tomonobu Hayashi, Carbonation of calcium silicate hydrates (C-S-H) having different calcium/silicon ratios, Semento, Konkurito Ronbunshu 43 (1989) 18–23.
[3] I.G. Richardson, G.W. Groves, A.R. Brough, et al., The carbonation of OPC and OPC/silica fume hardened cement pastes in air under conditions of fixed humidity, Adv. Cem. Res 5 (18) (1993) 81–86.
[4] Tadahiro Nishikawa, Kazutaka Suzuki, Carbonation of calcium silicate hydrate, Semento Konkuriito, vol. 528, 1991, pp. 32–39.
[5] K. Kobayashi, K. Suzuki, Y. Uno, Carbonation of concrete structures and decomposition of C-S-H, Cem. Concr. Res. 24 (1) (1994) 55–61.
[6] Sangkyu Kim, Hisashi Taguchi, Yoko Ohba, et al., Carbonation of calcium hydroxide and calcium silicate hydrates, Muki Materiaru 2 (254) (1995) 18–25.
[7] Geoffrey W. Groves, Adrian Brough, Ian G. Richardson, et al., Progressive changes in the structure of hardened C3S cement pastes due to carbonation, J. Am. Ceram. Soc. 74 (11) (1991) 2891–2896.
[8] G Sergi, "Corrosion of Steel in Concrete: Cement Matrix Variables. PhD thesis," Aston University, 1986.
[9] J.A. Gonzalez, S. Algaba, C. Andrade, Corrosion of reinforcing bars in carbonated concrete, Br. Corros. J. 15 (3) (1980) 135–139.
[10] C. Alonso, C. Andrade, Efecto que el tipo de cemento y la dosificación del mortero ejercen en la velocidad de corrosión de armaduras embebidas en mortero carbonatado, Mat. De Construc. 37 (205) (1987) 5–15.
[11] R.L. Berger, Stabilisation of silicate structure by carbonation, Cem. Concr. Res. 9 (5) (1979) 649–651.
[12] Z. Sauman, V. Lach, Long term carbonization of the phases 3CaO.Al2O3.6H2O and 3CaO.Al2O3.4H2O, Cem. Concr. Res. 2 (1972) 435–446.
[13] W.F. Cole, B. Kroone, Carbonate minerals in hydrated portland cement, Nature 4688 (1959) 59.

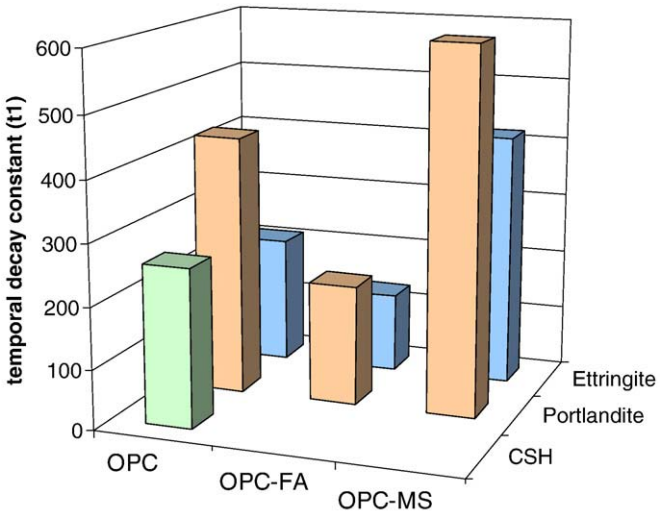

Fig. 11. Temporal decay constant t1, for the different phases and mixes during the carbonation process.

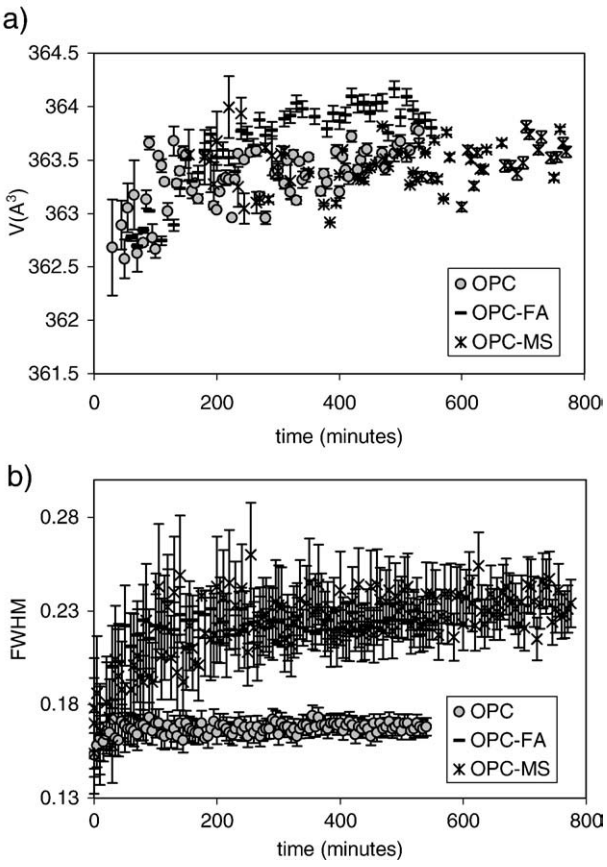

Fig. 12. (a–b). Evolution of the a) volume of the unit cell of calcite and b) FWHM as the carbonation treatment goes on.

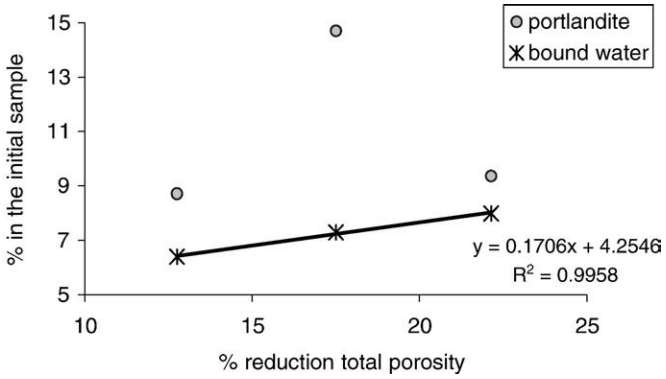

Fig. 13. Reduction in the total porosity (% vol) due to carbonation, and the initial percentage of Portlandite and bound water in the samples.

[14] W.F. Cole, B. Kroone, Carbon dioxide in hydrated portland cement, J. Am. Conc. Inst. 31 (1960) 1275–1295.
[15] S.E. Pihlajavaara, Same results of the effect of carbonation on the porosity and pore size distribution of cement paste, Mat. et Cons. 1 (6) (1968) 521–526.
[16] H.F.W. Taylor, Cement Chemistry, Academic Press, London, UK, 1990.
[17] S.E. Pihlajavaara, E. Pihlman, Effects of carbonation on microstructural properties of cement stone, Cem. Concr. Res. 4 (2) (1974) 149–154.
[18] B. Johannesson, P. Utgenannt, Microstructural changes caused by carbonation of cement mortar, Cem. Concr. Res. 31 (6) (2001) 925–931.
[19] V.T. Ngala, C.L. Page, Effects of carbonation on pore structure and diffusional properties of hydrated cement pastes, Cem. Concr. Res. 27 (7) (1997) 995–1007.
[20] L.J. Parrott, Carbonation, moisture and empty pores, Adv. Cem. Res 4 (15) (1992) 111–118.
[21] Y.F. Houst, F.H. Wittmann, Depth profiles of carbonates formed during natural carbonation, Cem. Concr. Res. 32 (2002) 1923–1930.
[22] M. Venuat, J. Alexandre, De la carbonatation du béton, Rev. Mater. Constr. (1968) 421–481.
[23] H. Weber, Methods for calculating the progress of carbonation and the associated life expectancy of reinforced concrete components, Betyonwerk+ Fertigteil-Technik, vol. 8, 1983, pp. 508–514.
[24] H.G. Smolczyck, "Discussions to M. Hamada's paper "Neutralization (carbonation) of concrete and corrosion of reinforcing steel"," presented at the Proc. 5th Int. Sym. Chem. Cem., Tokyo, 1968.
[25] M. Kokubu and S. Nagataki, "Carbonation of concrete with fly ash and corrosion of reinforcements in 20-years test," presented at the Third ICFSS, Trondheim, 1989.
[26] K. Tuuti, "Corrosion of Steel in Concrete, PhD thesis, Swedish Cement and Concrete Research Institute (CBI), Stockholm, 1982.
[27] R. Bakker, Prediction of service life reinforcement in concrete under different climatic conditions at given cover, corrosion and protection of steel in concrete, in: R.N. Swamy (Ed.), Int. conference, 1964, Sheffield.
[28] L.J. Parrot, Design for avoiding damage due to carbonation-included corosion-. SP-145-15, in: Malhotra (Ed.), Int. Congress on Durability of Concrete, CANMET, Nice, 1994, pp. 283–298.
[29] C. Andrade, C. Alonso, A. Arteaga, P. Tanner, Methodology based on the electrical resistivity for the calculation of reinforcement service life, in: V.M. Malhotra (Ed.), Proceedings of the 5th CANMET/ACI International Conference on Durability of Concrete, June 4–9, 2000, ACI, Barcelona, Spain, 2000, pp. 899–915, Supplementary paper.
[30] M.A. Sanjuan, C. Andrade, M. Cheyrezy, Concrete carbonation tests in natural and accelerated conditions, Adv. Cem. Res 15 (2003) 171–180 N° 4, October.
[31] M. Castellote, L. Fernandez, C. Andrade, C. Alonso, Chemical changes and phase analysis in carbonated OPC paste at different CO2 concentrations, Mat. Struct. (2008), doi:10.1617/s11527-008-9399-1.
[32] V.F. Sears, Neutron News 3 (1992) 29–37.
[33] G.L. Squires, Introduction to the Theory of Thermal Neutron Scattering, Cambridge Univ. Press, London, 1978.
[34] A.A. Rahman, F.P. Glasser, Comparative studies of the carbonation of hydrated cements, Adv. Cem. Res. 2 (6) (1989) 49–54.
[35] JCPDS International Centre for Diffraction Data (JCPDS-ICDD 2000): PDF number 35-0772; Natl. Bur. Stand. (US) Monogr. 25, 21, 72 (1985).
[36] International Tables for X-Ray Crystallography, Volume II, in: U. Shmueli (Ed.), Mathematical Tables, Kluwer Academic Publishers, Dordrecht, 1993.